Comparison of RANS CFD and lower-order aerodynamic models for 3D Vertical Axis Wind Turbines

Pierre-Luc Delafin[1]*, Takafumi Nishino [1], Lin Wang [1], Athanasios Kolios [1], Theodore Bird [2]

[1] Center for Offshore Renewable Energy Engineering, Cranfield University,
Cranfield, MK43 0AL, UK

[2] Aerogenerator Project Limited, Ballingdon Mill, Sudbury, CO10 7EZ, UK

1 Introduction

There was a large interest in Vertical Axis Wind Turbines (VAWT's) in the 1970s [1, 2] before the wind energy industry was developed and dominated by horizontal axis wind turbines. Recently, there is a resurgent interest in VAWT's especially for offshore applications [3, 4].

The aerodynamics of a VAWT is complicated because of the continuously varying blades' angle of attack and chord Reynolds number. Specific aerodynamic models are available for an efficient design of such turbines. For example, Double Multiple StreamTube (DMST) models [5] have been extensively developed and used for this purpose. They were considered for a long time as the "state-of-the-art" for VAWT's design. However, they nowadays receive some criticisms regarding the accuracy of their results, i.e. good agreements with experiments could result from cancellation of errors [6]. The aim of this study is to compare such aerodynamic models widely used for turbine design (DMST and vortex-based methods) with more time-consuming CFD calculations as well as with existing experimental data in order to evaluate the validity of each method.

2 Approach

2.1 Turbine

The turbine studied is the second version of the Sandia National Laboratories (SNL) 17m VAWT (Fig. 1). Each blade consists of three sections (straight/circular/straight) approximating a Troposkein shape. Experimental data can be found in Sandia technical reports [7, 8]. The main geometric parameters are summarized in Table 1. In this study, we focus on the rotational speed of 50.6 rpm.

2.2 Aerodynamic models

2.2.1 TM4E: Turbine Model version 4E

TM4E is based on the DMST method and automatically divides the turbine height into 200 layers for the calculation of the induced velocities [9].

2.2.2 CACTUS: Code for Axial and Cross-flow TUrbine Simulation

CACTUS is a three-dimensional free-vortex code using the lifting line approximation to model the blades [10]. Following the results of a convergence study, each blade is represented by 27 elements and 40 time steps are used per revolution. Calculations are run for 10 turbine revolutions which leads to a

---

*Presenting author. Email address: p.p.delafin@cranfield.ac.uk

Figure 1: SNL 17m Darrieus vertical axis wind turbine [7].

Height (m)	17
Diameter (m)	16.7
Number of blades	2
Swept area (m^2)	187
Aerofoil	NACA 0015
Chord length (m)	0.61
Solidity	0.16
Ground clearance (m)	4.88
Operating speed (rpm)	29.8 - 54.8
Generator (kW)	55.9

Table 1: SNL 17m vertical axis wind turbine specifications [8].

good level of convergence (deviation of the power coefficient CP is less than 0.8% between the last two revolutions).

2.2.3 ANSYS CFX (CFD)

Incompressible Reynolds Averaged Navier Stokes (RANS) equations are solved using ANSYS CFX [11]. The k-omega SST (Shear Stress Transport) turbulence model [12] is used to model the Reynolds shear stress. This turbulence model is known to be suitable for lifting bodies applications with adverse pressure gradients.

We use a structured grid, which is divided into two parts (Fig. 2):

- A rotating cylindrical domain (rotor) containing the turbine. The diameter of this cylindrical domain is 50m (turbine diameter D = 17m) with a height of 19m (turbine height is 17m). This domain consists of approximately 7×10^6 cells.

- A rectangular outer domain (stator) of length 60D, width 60D and height 11D. The outer domain consists of approximately 2×10^6 cells.

A transient rotor-stator interface using the GGI (General Grid Interface) method is employed between the rotor and the stator. Fig. 3 shows the mesh around the turbine in the equatorial plane. The mesh has been refined close to the blades to reach the target $y^+_{max} \sim 1$ to resolve the viscous sublayer sufficiently.
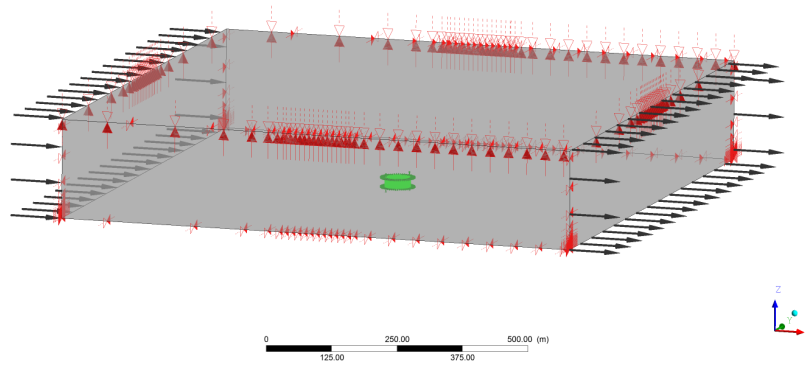
Figure 2: Computational domain consisting of rotor (green) and stator (grey) sub-domains.
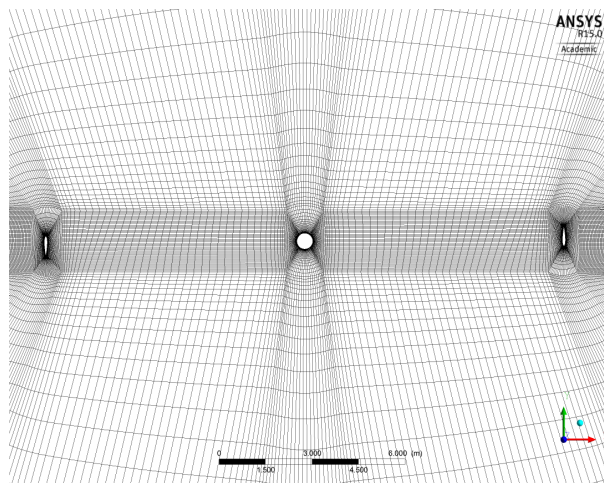
Figure 3: View of the structured grid around the turbine in the equatorial plane.

Each blade is represented by 140 nodes in the chordwise direction (suction and pressure sides) and 145 nodes in the spanwise direction.

All calculations use a time step corresponding to an azimuthal variation of 1°. The atmospheric boundary layer is taken into account by specifying a power law velocity profile at the inlet boundary. As mentioned in the Sandia report [13], the reference height is 13.5m and the exponent is 0.1 (the bottom of the turbine is placed 5m above the ground). The density of air is 1.0 kg/m^3 as measured at the test facility located at a high altitude.

3 Results and discussion

3.1 Averaged performance

Results of power plotted as a function of the wind speed are presented in Fig. 4 (left). TM4E calculations tend to over-predict the power but give a similar slope to the experimental data. CACTUS results show a slight improvement compared to the TM4E results at low wind speeds but are very similar at high wind speed. CFD results show a very good agreement with the experiments for the three wind speeds considered (7m/s, 9.8m/s and 15.7m/s).

The variations of CP with the tip speed ratio (TSR) are plotted in Fig. 4 (right). The agreement between the experiments and TM4E calculations is good for TSR < 4 but a significant difference is observed for TSR > 4. This large difference in CP is essentially due to the low power values obtained

at high TSR's. The results shown here are for a constant rotational speed and hence the high TSR's correspond to low wind speeds. Therefore a small difference in power at low wind speeds leads to a large difference in CP at high TSR's. CFD calculations show very good agreements with the experiments at TSR = 2.9 and 4.6. A slight over-prediction can be observed at TSR = 6.4.
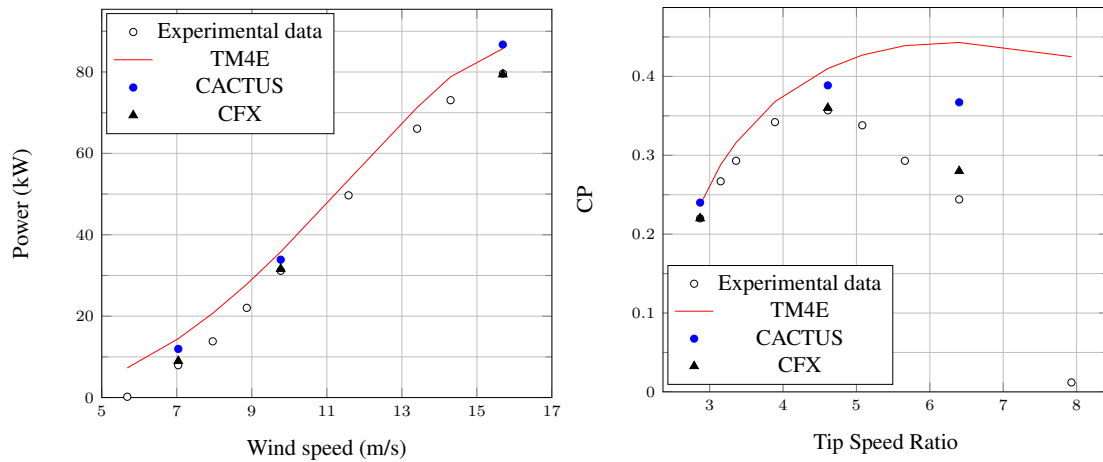
Figure 4: Power vs wind speed (Left) and Power Coefficient vs Tip Speed Ratio (Right), for a constant rotational speed of 50.6rpm.

3.2 Flow field

CFD calculations give information about the flow field inside and around the turbine. Contours of the normalised streamwise velocity in the equatorial plane are plotted in Fig. 5 for three different tip speed ratios. The wake of the central tower can be seen for all three cases. However, the (normalised) velocity inside and behind the entire turbine depends significantly on the tip speed ratio, i.e. the velocity decreases as the tip speed ratio increases, affecting the aerodynamic performance of the blades travelling through the downstream half of the turbine.
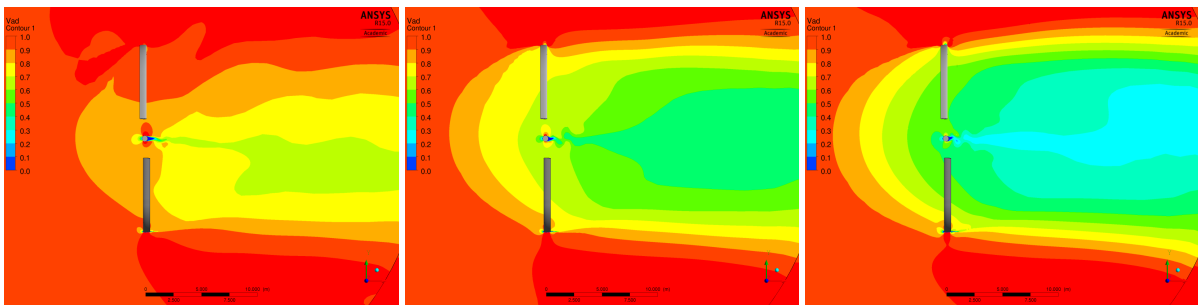
Figure 5: Contours of normalised streamwise velocity (U_x/U_∞) in the equatorial plane at tip speed ratios of 2.9 (left), 4.6 (middle) and 6.4 (right).

3.3 Instantaneous turbine torque

The evolution of turbine torque with the azimuthal angle is plotted in Fig. 6, 7 and 8 corresponding to TSR = 2.9, 4.6 and 6.4 respectively. The torque is plotted for only one half of the revolution assuming symmetry of the torque evolution for the 2-blade turbine. TM4E calculations significantly over-predict the torque generated by the turbine for azimuthal angles in the range of 60° to 120°. The agreement is better close to the azimuth 0° and 180°. CACTUS results show a better agreement with the experiments than the TM4E calculations but slightly over-predict the maximum torque. CFD results show a better

4

agreement with the experiments than CACTUS calculations. However, the maximum torque is predicted with a delay of 10° to 20° of azimuth compared to the experiments.
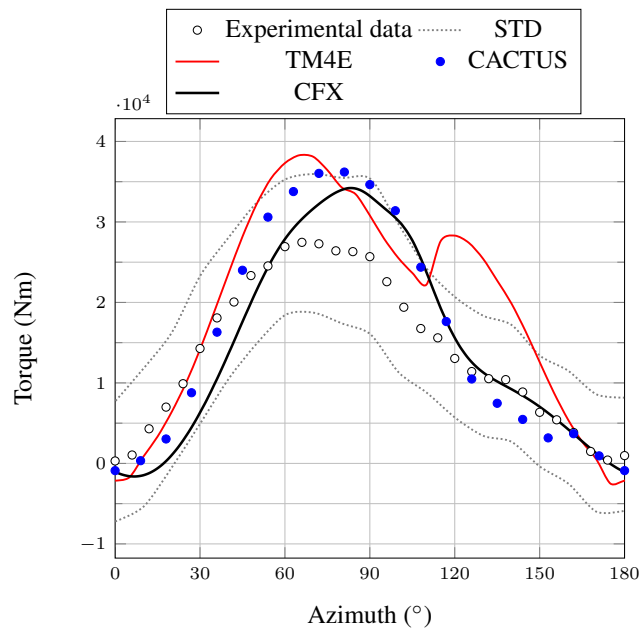
Figure 6: Instantaneous torque plotted for half a revolution, TSR = 2.9. STD = Standard deviation of experimental data.
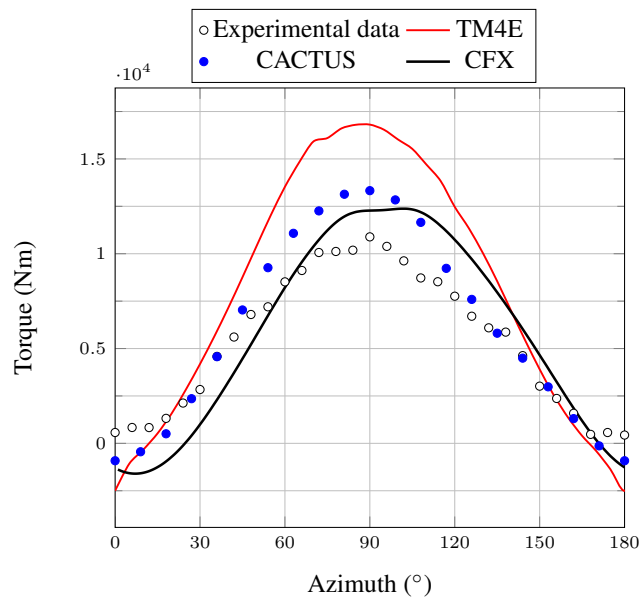
Figure 7: Instantaneous torque plotted for half a revolution, TSR = 4.6.
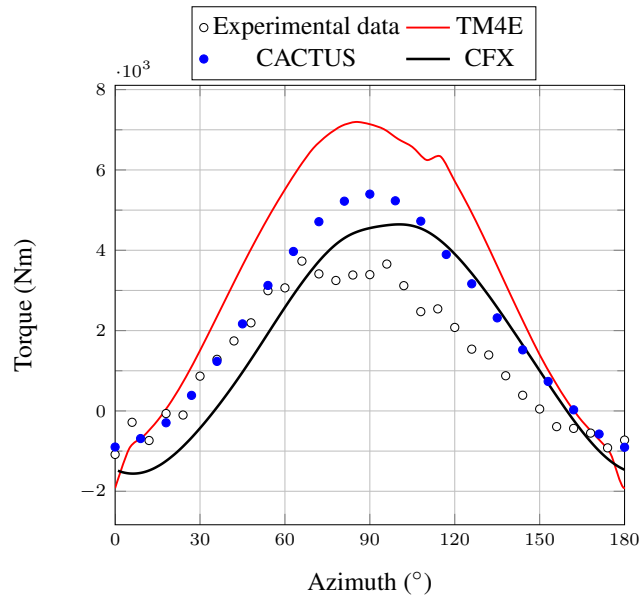
Figure 8: Instantaneous torque plotted for half a revolution, TSR = 6.4.

4   Conclusion

We have compared two different aerodynamic models commonly used in vertical axis wind turbine design (DMST and vortex methods) with RANS CFD calculations and existing experimental data for the Sandia 17m Darrieus turbine. As expected, the DMST method was shown to be less accurate than the vortex method, which itself was shown to be less accurate than the RANS CFD. For all tip speed ratios tested, the DMST method significantly over-predicted the torque amplitude whereas the RANS CFD gave a good prediction of this amplitude.

The Sandia experimental data used in this study enabled detailed comparisons at three different operating points (before, after and at the maximum efficiency). However, no data were available for very low tip speed ratios at which the blades would experience deep dynamic stall.

5   Learning objectives

In this work, the following learning objectives have been achieved:

- To establish a CFD model of a full-scale vertical axis wind turbine;

- To compare widely used aerodynamic models (DMST and Vortex based methods) with CFD and Sandia experimental data;

- To compare power, power coefficient and instantaneous torque for three operating conditions (before, after and at the maximum efficiency).

6   Acknowledgements

References

[1] H. Sutherland, D. Berg, and T. Ashwill. A Retrospective of VAWT Technology. Technical Report SAND2012-0304, SANDIA, 2012.

[2] R. Templin. Aerodynamic Performance Theory for the NRC Vertical-Axis Wind Turbine. Technical Report Rept. LTR-LA-160, 1974.

[3] B.Owens and D. Griffith. Aeroelastic Stability Investigation for Large-Scale Vertical Axis Wind Turbines. The Science of Making Torque From Wind, 2014.

[4] U. Paulsen, H. Madsen, J. Hattel, I. Baran, and P. Nielsen. Design Optimization of a 5 MW Floating Offshore Vertical-Axis Wind Turbine. DeepWind'2013, 2013.

[5] I. Paraschivoiu. Double-Multiple Streamtube Model for Studying Vertical-Axis Wind Turbines. *Journal of Propulsion and Power*, pages 370–377, 1988.

[6] C. Simao Ferreira, H. Aagaard Madsen, M. Barone, B. Roscher, P. Deglaire, and I. Arduin. Comparison of Aerodynamic Models for Vertical Axis Wind Turbines. The Science of Making Torque From Wind, 2014.

[7] R. Akins, D. Berg, and W. Cyrus. Measurements and Calculations of Aerodynamic Torques for a Vertical-Axis Wind Turbine. Technical Report SAND86-2164, SANDIA, 1987.

[8] M. Worstell. Aerodynamic Performance of the DOE/Sandia 17-m Diameter Vertical Axis Wind Turbine. *Journal of Energy*, pages 39–42, 1981.

[9] A. Shires. Development and Evaluation of an Aerodynamic Model for a Novel Vertical Axis Wind Turbine Concept. *Energies*, pages 2501–2520, 2013.

[10] J. Murray and M. Barone. The Development of CACTUS, a Wind and Marine Turbine Performance Simulation Code. 49th AIAA Aerospace Sciences Meeting, 2011.

[11] CFX. *ANSYS CFX Solver Theory Guide*, volume 14.0. ANSYS, 2011.

[12] F.R. Menter. Two-Equation Eddy-Viscosity Turbulence Models for Engineering Applications. *AIAA Journal*, 32(8):1598–1604, August 1994.

[13] M. Worstell. Aerodynamic Performance of the 17 Meter Diameter Darrieus Wind Turbine. Technical Report SAND78-1737, SANDIA, 1978.